

Non-Optical Applications of Photonic Crystal Structures

A Report to the US Air Force Office of Scientific Research

Alexander J. Glass, Ph.D.

University of New Mexico

DISTRIBUTION STATEMENT A
Approved for Public Release
Distribution Unlimited

Ajglass2002@yahoo.com

23 February 2005

20051013 169

Non-Optical Applications of Photonic Crystal Structures

Alexander J. Glass, Ph.D.

University of New Mexico

I. Introduction

The propagation of waves in periodic structures was first analyzed in detail by Leon Brillouin, in his early book, *Quantenstatistik*¹, and in his comprehensive volume, *Wave Propagation in Periodic Structures*². The unique properties that arise from the interaction of a periodic disturbance (a wave) and a periodic structure, such as a crystal lattice, are primarily manifested only when the wavelength of the disturbance is comparable to the lattice spacing. In most natural crystals, the lattice spacing is typically a fraction of a nanometer, corresponding to the wavelength of an electron in a conduction state. Thus, the well-known band theory of electronic conduction in solids³ was one of the first applications of Brillouin's work in more than one dimension. (Electrical circuits and transmission lines provide one-dimensional examples of wave propagation in a periodic medium.)

As the technology of synthetic materials advanced, it became possible to construct periodic structures with lattice spacing comparable to the wavelength of light. The foremost example of this approach is the manufacture of multi-layer dielectric coatings for use in optical systems⁴. Alternate layers of high and low-index materials are deposited on the surface of an optical element to control the reflection and transmission of light. Anti-reflection coatings based on optical interference were first developed by Smakula⁵ at Carl Zeiss, Inc. in 1936, and the technology of multiplayer coatings developed greatly during the second World War, as both sides sought to improve the performance of optical devices. Further advances in micro-fabrication accompanied the development of microprocessors and large-scale electronic integration. By the late 1980s, the capability existed to manufacture entirely new materials ("meta-materials") with complex internal structures on any scale, from individual atom size up to optical wavelengths and beyond.

The field of photonic crystals was launched with the publication by Eli Yablonovich^{6,7} in 1987 of a paper on inhibition of spontaneous emission in a three-dimensional periodic structure, followed shortly by a discussion of a possible realization of a material displaying a three-dimensional photonic band gap. About the same time, Phillip Russell⁸ and co-workers introduced the concept of "photonic crystal fibers," optical fibers drawn with a specifically structured cross-section that limits the propagation of light to certain bands of frequencies. Again, this technology was enabled by advances in the fabrication of fiber optics, and takes advantage of the extreme flexibility of design afforded by the properties of silicate glass.

An extensive bibliography of books, reports and papers dealing with photonic crystals and related topics has been placed on the Internet by Prof. Jonathan Dowling at Louisiana State University⁹. The bibliography contains 6 references to computer codes, 40 references to books and special journal issues, 79 references to special reports, 4851 journal citations, and 140 references to sonic band gap materials (phononic crystals).

The literature on band gap materials has grown exponentially since 1987. The accompanying figure, taken from Dowling's bibliography, shows the growth of photonic band gap publications from 1987 to 2002. The growth curve is well modeled by the expression, $N = 6 \cdot \exp((\text{year} - 1987)/3)$.

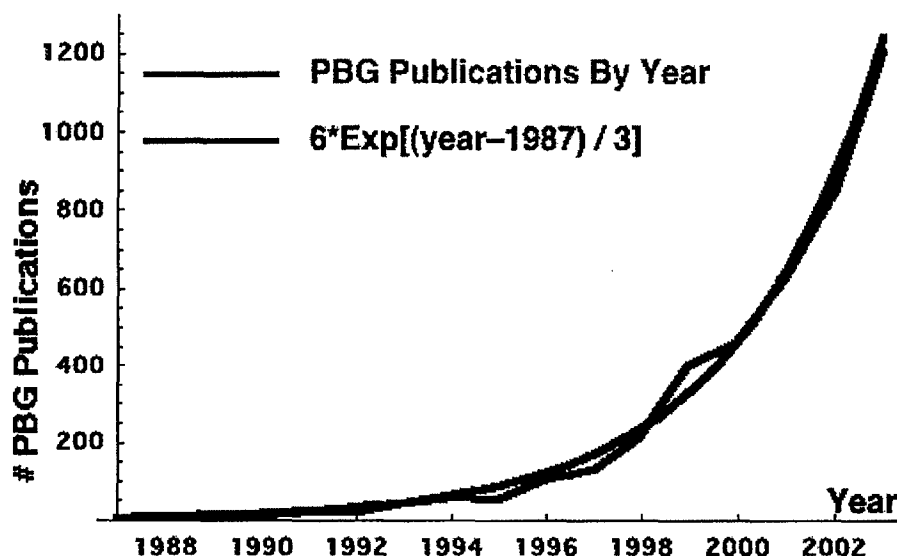


Fig. 1 – Growth of Photonic Band Gap Publications

Many of the primary applications of photonic crystal structures are in the optical frequency range (400nm to 10 μm). Two-dimensional structures – both photonic crystal fibers and planar, integrated photonic circuit elements, have attracted a great deal of attention. Because of the potential to limit the phase space for the optical decay of excited atoms, three-dimensional photonic crystals have attracted significant interest for basic physics investigations.

Designing and fabricating structures on the scale of fractions of a μm , especially in two or three dimensions, requires precision equipment and careful assembly. For research purposes, many investigators chose to test their concepts at the more convenient and forgiving scale of short wavelength radio frequencies – millimeter waves or microwaves. Thus, in their early paper on face-centered-cubic photonic crystal structures, Yablonovich and Gmitter⁷ constructed and evaluated a number of models for fcc structures, on the microwave scale (1-20 GHz), using an array of spherical voids (filled with air) in a matrix of low-loss dielectric (microwave refractive index = 3.5). Three-dimensional arrays could be fabricated using conventional machining techniques. Thus, empirical investigations, involving cut-and-try experimentation, could be carried out quickly and at reasonable cost to prove concepts and design materials for use in the optical regime. Regarding operating in the microwave regime, the authors commented:

“We have elected to do our initial experimental work at microwave frequencies, where the periodic dielectric structures can be fabricated by conventional machine tools. Furthermore, this has enabled us to use sophisticated microwave homodyne detection techniques to measure the phase and amplitude of the electromagnetic Bloch functions propagating through the ‘Photonic Crystal’.”

Operating at microwave frequencies not only offers advantages in terms of simpler fabrication, but also of real practical applications. As we shall see, photonic crystal structures can be used to improve the directionality of antennas, reduce surface losses, and otherwise improve the radiation efficiency of microwave devices. Similarly, it was quickly recognized that photonic crystals had applications for Terahertz (THz) waves, with wavelengths in the range of 10-1000 μm . Manufacturing techniques in this range of dimensions have been developed for MEMS devices, and can be applied to the construction of two and three-dimensional photonic crystals for THz applications.

Although not governed by Maxwell's equations, acoustical, elastic and seismic waves all exhibit the phenomena of diffraction, scattering, and interference. Sound speeds vary from 330 m/s in air to 12,900 m/s in beryllium, so wavelengths in the audible range (10-20,000 Hz) are measured in cm to meters. Phononic crystals (the acoustical analogue of photonic crystals) in this frequency range are large devices. However, in the ultrasonic range, with frequencies of 100 kHz to 10 MHz, wavelengths are again in the range of 100 μm to a few cm in most materials.

In this report, we will consider applications of photonic (phononic) crystal structures to microwave, mm-wave, and THz electromagnetic waves, and acoustic and ultrasonic waves. We will briefly discuss recent experiments relating to seismic and water waves as well.

II. Basic Principles

Photonic crystals are periodic structures with a period comparable to the wavelength of the propagating wave. If the wavelength is much longer than the period of the crystal, the interaction of the wave and the material can be treated using an average index approximation. If the wavelength is much shorter than the crystal period, scattering can occur at the interfaces, but resonant scattering can only occur if the coherence length of the wave is significantly greater than the crystal spacing. The special properties of photonic crystals, especially the appearance of "stop bands" in which waves of a certain frequency cannot propagate, arise from the interference of waves scattered from a succession of equally spaced interfaces.

For purposes of illustration, it is useful to consider a scalar wave propagating in a one-dimensional periodic structure. The wave propagates according to the scalar wave equation, which, for a monochromatic wave of frequency ω , is:

$$f_{xx} + (n\omega/c)^2 f = 0 \quad (1)$$

Here n is the refractive index of the medium, and c/n is the local wave velocity. If the medium is periodic, the wave function f must take the form of a Bloch¹⁰ mode,

$$f(x) = u_K(x) e^{iKx} \quad (2)$$

The Bloch mode expresses the fact that, apart from a phase factor, the wave function is invariant under translations of an integer multiple of the lattice spacing. Thus the problem is completely described by the solution in a single "unit cell." For a given frequency ω , the propagation factor K is uniquely specified, giving rise to a dispersion relation, $K(\omega)$. The solution of the wave equation for a periodic structure can be rewritten as an eigenvalue problem, where $u_K(x)$ is the eigenfunction and $K(\omega)$ is the corresponding eigenvalue. The variational statement of the problem can be used to find an iterative algorithm for the numerical solution of wave

propagation problems in complex, multi-dimensional photonic crystal designs (See Appendix D of the monograph on photonic crystals by Joannopoulos, Meade, and Winn¹¹)

An illustrative example of how the introduction of a periodic structure gives rise to pass bands and stop bands is provided by the Kronig-Penney (KP) model¹². The KP model consists of alternate layers of material in which the index n takes on different values.

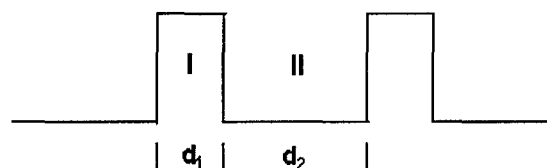


Fig. 2 Kronig-Penney Model

In the accompanying figure, the wave velocity in region I is c/n_1 , and in region II is c/n_2 , and the propagation constant is $k_1 = n_1 \omega/c$ in region I and $k_2 = n_2 \omega/c$ in region II. Introducing the following symbols:

$$\begin{aligned}\Delta &= k_1 d_1 + k_2 d_2 \\ \delta &= k_1 d_1 - k_2 d_2\end{aligned}\tag{3}$$

$$\mu = k_2 / k_1$$

At frequency ω , the dispersion relation $K(\omega)$ becomes:

$$\cos Kd = (\cos \Delta)(1 + \eta) - \eta \cos \delta\tag{4}$$

where:

$$\eta = (\mu - 1)^2 / 4 \mu\tag{5}$$

It is immediately apparent from Eq. 4 that waves cannot propagate through the structure unless $(-1 < \cos Kd < 1)$. The first gap in the spectrum of propagating frequencies occurs when $\Delta \sim \pi$, at which point $\cos \Delta = -1$ and $\cos Kd < -1$. Subsequent band gaps appear at each resonance, where $\Delta \sim n\pi$. Fig. 3 shows a typical band structure for the KP model. The vertical axis is in units of Δ , which is proportional to the signal frequency. Stop bands are indicated by solid lines along the vertical axis.

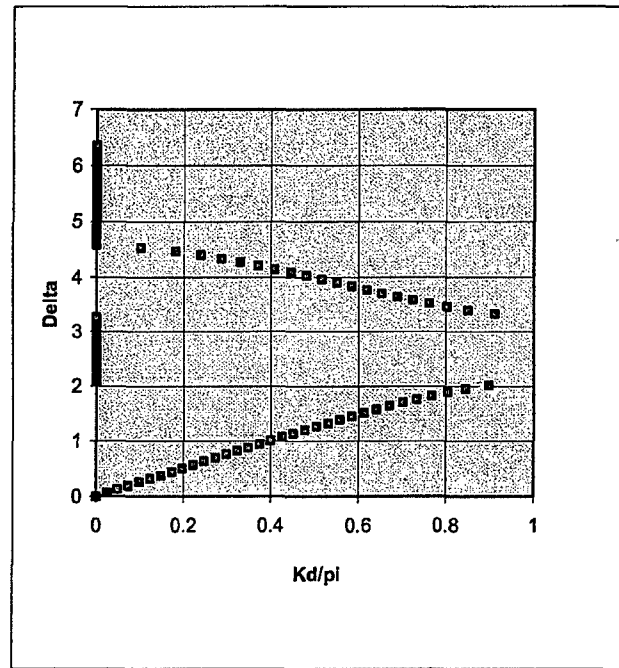


Fig. 3 – Band Structure of Kronig-Penney Model

Specific examples of one-dimensional band structures in KP models can be found in Chapter 4 of Ref. 11. A detailed analysis of the Kronig-Penney model has recently been published¹³ that includes a discussion of both longitudinal and transverse propagating modes and the effects of off-axis incidence.

Fig. 3 shows only the first two stop bands of the KP model. Much more complex diagrams are obtained for multi-dimensional structures. It is customary to display the dispersion relation in a two-dimensional plot showing the frequency vs. the magnitude of the Bloch \mathbf{k} -vector for various directions in the crystal, as is shown in Fig. 4. This kind of diagram is widely used to explain electronic conduction in crystals. Fig. 4 shows the dispersion diagram for a two-dimensional structure¹⁴ with a square lattice. We see that there are ranges of frequencies in which there is no propagating mode in any direction, *i.e.*, a complete band gap. At other frequencies, there are certain directions in which propagation in the crystal is forbidden, but allowed in other directions. The structure of the dispersion relation is made clearer by showing the three dimensional dispersion surfaces, as in Fig 5. The stop band in the range $(0.4 < (\omega d/2\pi c) < 0.5)$ is clearly observable. It is also dramatically clear that in certain directions in the crystal, the group velocity, $\nabla_{\mathbf{k}}(\omega)$, can be zero or negative. Due to the strong variation of group velocity, especially near the edge of the stop bands, waves in photonic crystal structures can display a wide variety of esoteric propagation characteristics¹⁵.

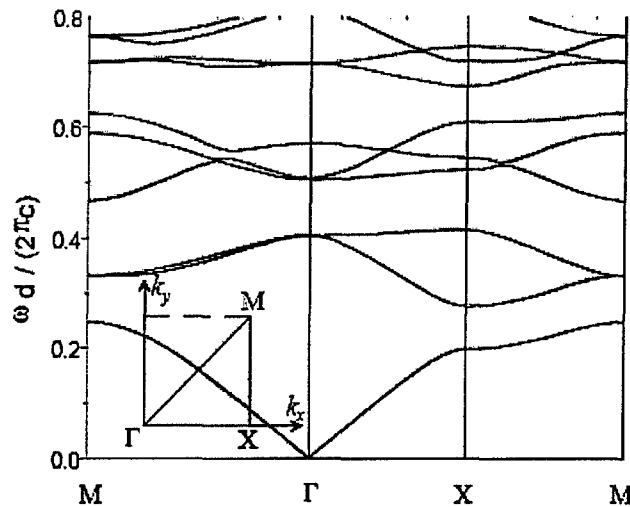


Fig. 4 – Dispersion diagram for E// polarization in a 2D crystal with square lattice. The abscissa represents the Bloch wave vector on the edge of the first reduced Brillouin zone shown in the small insert: Γ , X and M stand for the points with coordinates $(0,0)$, $(\pi/d, 0)$ and $(\pi/d, \pi/d)$ in the (k_x, k_y) plane.

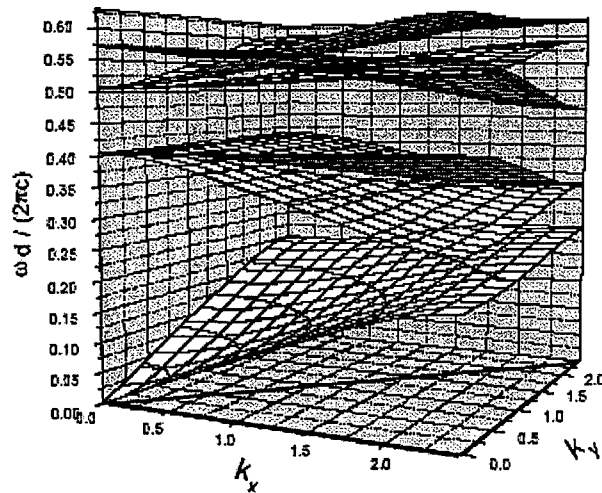


Fig. 5 – Three-dimensional dispersion diagram. The horizontal plane gives the Bloch wave vector \mathbf{k} . The vertical axis gives the normalized frequency $\omega d/(2\pi c) = d/\lambda$. The bottom sides of the sheets are represented in darker gray. The triangle corresponding to the first reduced Brillouin zone has been drawn in the (k_x, k_y) plane. The parameters are the same as in figure 4.

The band structure shown above is idealized, and only applies strictly to periodic structures of infinite extent. In reality, radiation will not be completely blocked in the stop bands, due to the effects of the finite extent of the lattice, and also of the presence of defects and imperfections in the structure. As with electrons in semiconductor materials, new phenomena arise due to these effects. For example, defects can give rise to localized allowed modes in the midst of a forbidden band. Impurity and defect modes are discussed in various parts of Ref. 11.

In what follows, we will not go into detail concerning computational methods. Simply stated, there are two commonly used approaches to modeling photonic crystal structures. Both start with the "Master Equation," which for electromagnetic problems is obtained from Maxwell's equations as:

$$\text{Curl} [(\text{curl } \mathbf{H}(\mathbf{r}))/\epsilon(\mathbf{r})] = (\omega/c)^2 \mathbf{H}(\mathbf{r}), \quad (6)$$

where Maxwell's equations have been written in the frequency domain. For acoustics problems, the master equation is written:

$$\lambda \text{ div} \cdot [(\text{grad } P)/\rho] = -\omega^2 P \quad (7)$$

As in the Kronig-Penney model, we invoke the Bloch theorem, and look for solutions that are periodic in space, with a periodicity given by the functional form, $\exp(i\mathbf{k} \cdot \mathbf{r})$. Then we seek the dispersion relation in the form $\omega(\mathbf{k})$. The dispersion relation is an expression of the eigenvalues of the master equation as \mathbf{k} is varied over all directions in the crystal. To obtain the eigenvalues, the master equation is usually converted to a variational problem and solved by conventional matrix methods. The calculation is straightforward, but requires a large number of basis functions to obtain the band structure accurately.

The other approach is to view the master equation as a propagation problem in the time domain, and solve the initial condition problem for the geometry under investigation. This method is more suited to analysis of finite structures and structures containing defects. The most common method used to solve the propagation equation is the Finite Difference Time Domain (FDTD) method. A summary of various computational methods can be found in the book¹⁶, *Electromagnetic Applications of Photonic Band Gap Materials and Structures*.

A general analysis of wave propagation in periodic structures has been carried out¹⁷ by Economou and Sigalas, in Greece. They contrast the two possible topologies of band gap materials, a) *Cermets*, in which the scattering medium (low-velocity) is distributed in isolated inclusions surrounded by the host medium (high-velocity), and b) *Networks*, in which the scattering medium inclusions are connected, and form a continuous network throughout the host material. The two topologies are analyzed for both the electromagnetic and acoustic master equations. For acoustic (and elastic) waves, they find that the cermet topology is more favorable for the formation of spectral gaps (stop bands), whereas for the electromagnetic case, the network topology is more favorable. They offer general rules relating the fractional bandwidth of and the upper frequency of the first stop band to the fill factor and velocity ratio of the two media.

III. Microwave Applications

Because of the difficulties in fabricating photonic crystal structures at the scale of an optical wavelength, much of the experimental work has been done using microwaves. At microwave frequencies (3-300 GHz) wavelengths are measured in cm or mm, so conventional machining techniques can be used to fabricate components. Dielectric materials exhibit high refractive indices at these frequencies, and additionally, metallic components can be used, adding another dimension to the design space. In addition, structure can be added to the individual elements of a

photonic crystal array, so that each component of the array becomes a circuit element, with an adjustable capacitance and inductance.

An extensive review of potential microwave applications of band-gap materials can be found in a special issue of Transactions on Microwave Theory and Techniques published in 1999. In that publication, Dan Sievenpiper¹⁸ *et al* discussed the improved performance of a microwave antenna mounted above a photonic crystal ground plane. In the band gap of the photonic crystal, the surface impedance of the ground plane is very high, suppressing surface currents, and eliminating multipath interference and backward radiation. The authors constructed their ground plane as a two-dimensional array of lumped-circuit elements, as is shown in Fig 6.

Three-Layer High-Impedance Surface

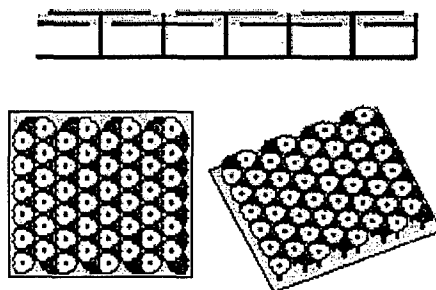


Fig. 6 – Three-Layer High-Impedance Surface

The resonance frequency of this structure is determined by the capacitance and inductance of each of the elements of the array. Increasing the capacitance of each element reduces the resonance frequency. At low frequencies, only the TM mode propagates on the surface. Above the band gap, TE modes propagate. Both modes are suppressed within the band gap.

In experiments with both monopole and patch antennas, significant differences were observed between the radiation pattern with a flat metal ground plane and a high-impedance, structured ground plane. Within the stop band of the ground plane, the radiation pattern is smoother, due to the suppression of multipath interference from surface waves. The radiation is also more directional, with at least 10 dB reduction in the backward direction. Outside the stop band, antenna performance is the same with either ground plane.

Sievenpiper *et al* also addressed a very practical problem of backward radiation from cell phones. They modeled the head of a cell phone user by a jar of tap water of 15 cm diameter and 20 cm tall. A ground plane was placed between a cell phone antenna and the water. Using a flat metal sheet as the reflector is impractical, because it must be spaced one-quarter wavelength from the antenna to avoid interference. A high-impedance plane, however, can be located directly adjacent to the antenna, and strongly suppresses radiation in the back direction, and surface current leakage to the back of the plane. Without the high-impedance back plane, the cell phone user can absorb as much as half the cell phone radiation. Independent of any supposed health effects, this represents a significant loss of efficiency for the cell phone. However, this energy is regained by inserting the high-impedance plane between the user and the antenna. Since the backward radiation is suppressed, the forward gain of the antenna is increased by 3 dB.

Cell phone manufacturers have not adopted the practice of using a high-impedance back plane to shield cell phone users, however¹⁹. Apparently, they concluded that it would add an unacceptable amount to the cost and size of cell phones.

Several other authors have explored the use of high-Z surfaces to improve antenna performance^{20,21}. As the authors of Ref 19 point out, "The microstrip patch antenna is a very popular design, because of its low profile, it can be non-planar, is easy to manufacture, and is inexpensive and robust." Patch antenna performance, however, is limited by surface wave losses and interference. The use of a band-gap material to create a high-impedance back plane allows the antenna to be placed directly on the back plane, to make a more compact package. Suppression of the surface current leads to a more directional radiation pattern, and suppression of side lobes due to interference.

Gonzalo *et al*²² tested the performance of a patch antenna mounted directly on a photonic crystal substrate formed by a square array of air columns embedded in a dielectric matrix. (see Figs. 7 and 8). The performance of this configuration was compared to that of the same antenna mounted on a conventional dielectric substrate. The band gap of the photonic crystal substrate extended from 13.5 GHz to nearly 16 GHz.

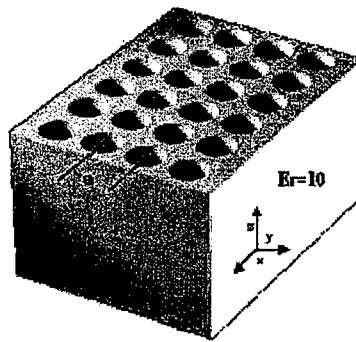


Fig. 7 – 2-D Photonic Crystal formed by a square array of air columns embedded in a dielectric substrate

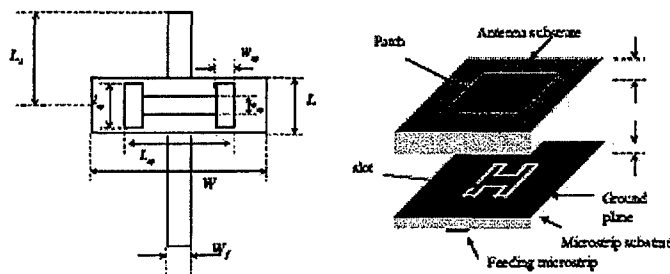


Fig. 8 – Geometry of the reference aperture coupling-fed patch antenna. The feeding line is a standard 50- Ω microstrip line on a dielectric substrate with thickness = 0.635 mm, relative permittivity = 10.2. Other dimensions are: $W = 4.6$ mm, $L = 1.5$ mm, other dimensions to scale.

Tests were conducted at a frequency at which the surface wave mode is added in opposite phase to the antenna, leading to a reduced gain in the boresight direction. This cancellation effect was almost completely eliminated by using the photonic crystal substrate, and the boresight gain was increased by more than 6 dB. The observed radiation pattern was smoother, and the side lobes were reduced. As long as operation was confined to frequencies within the band gap, the radiation pattern did not vary with frequency, whereas with the conventional substrate, strong variation was observed. This is to be expected, since in this case, the radiation pattern is strongly affected by interference effects, which change with frequency.

Lin *et al*²³ found further improvement by placing a photonic band gap cover over the patch antenna. In the band gap, the radiation cannot propagate across the cover. The field distribution on the cover surface is quite uniform, and the cover acts like an extended aperture antenna, reducing the angular divergence of the emitted radiation. For an aperture area of 145 mm x 145 mm, operating at 2.3 GHz, the bare patch antenna produced a directivity of 4.3 dB. Adding a band-gap back plane raised the directivity to 5.0 dB. Adding the photonic bandgap cover raised the directivity to 10.4 dB, close to the theoretical limit of 12.0 dB for the aperture size.

Recently, Sievenpiper²⁴ *et al* have described an electronically steerable antenna created by covering a metallic ground plane with a periodic band-gap structure. By incorporating varactor diodes into the structure, they have built a tunable impedance surface, in which an applied bias voltage controls the resonance frequency and the reflection phase. The surface can be programmed to create a tunable phase gradient, which can electronically steer a reflected beam over $\pm 40^\circ$ in two dimensions, for both polarizations. This type of resonant surface texture can provide greater bandwidth than conventional reflectarray structures, and offers a low-cost alternative to a conventional phased array.

A further advantage of the high-impedance substrate was pointed out by Yang and Rahmat-Samii²⁵. They mounted two microstrip antennas on a common substrate, and measured the mutual coupling, with and without a band-gap structure between them. The band gap structure was similar to that shown in Fig. 6, above. With no band-gap structure between the antennas, mutual coupling was -16.8 dB. With the band-gap strip inserted between the antennas, the mutual coupling was reduced to -24.6 dB. These experimental results were in good agreement with numerical simulations. The simulations also showed that if the antenna was operated at a frequency outside the stop band, the band-gap structure was not effective in reducing the mutual coupling. The authors propose that this technique could be effective in improving the performance of microstrip antenna arrays.

The high-impedance substrates described above entail construction of a three-dimensional structure, either by drilling holes in a dielectric slab, or by covering the surface with an array of thumbtack-like metallic pedestals. These can be readily fabricated using printed circuit board technology, but added steps in fabrication lead to added cost. A recent paper²⁶ shows that band-gap materials can be fabricated by depositing an array of metallic elements on the surface of a dielectric substrate. Each element can be tailored for a specific inductance and capacitance. The use of a periodic network of LC elements shortens the wavelength (slows the propagation velocity) of the propagating wave, leading to a more compact structure. The resulting planar structure offers the advantage of compatibility with standard planar circuit technology. Effective band-gap performance was observed in the frequency range around 10 GHz. This structure was recently shown²⁷ to be effective in reducing ground-bounce noise, which is a major concern for high-speed digital circuits.

Professor Ekmel Ozbay and his colleagues at Bilkent University in Turkey have carried out an extensive program of research on microwave applications of band-gap structures²⁸. Much of their research has made use of the “log-pile” structure²⁹ shown in Fig 9a. (This structure is also called a “layer-by-layer” photonic band gap crystal.) It is one of several three-dimensional structures that exhibit a “complete” band-gap, a range of frequencies in which propagation is forbidden in all directions. This particular structure has the advantage of being easy to fabricate. In this case, the structure is made of alumina rods separated by air. As is shown in Fig 9c, a band-gap is observed for frequencies from 10 to 16 GHz. Removing either a rod or a plane from the stack creates a defect in the crystal structure, and a new, narrow pass band is associated with the defect, as is seen in Fig 9d.

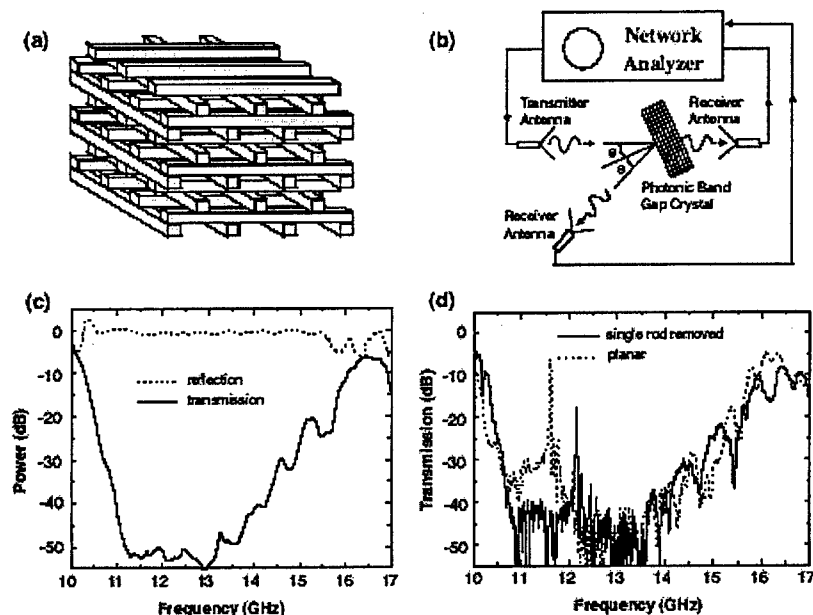


Fig. 9 – (a) Schematics of a three-dimensional layer-by-layer photonic crystal. (b) The experimental setup for measuring the transmission and reflection characteristics of the photonic crystal. (c) Transmission (solid line) and reflection (dotted line) profiles of 4-unit cell periodic structure along the stacking direction. (d) Transmission characteristics of a single rod removed (solid line) and planar (dotted line) defect structures.

Using this structure, Professor Ozbay’s group demonstrated both linear and L-shaped waveguides for microwaves in the 10-13 GHz range. As expected the waveguides are highly dispersive near the band edges, and the L-shaped guide only transmitted 35% of the incident radiation.

They also demonstrated an alternative means of guiding waves through band-gap material, by creating a series of localized defect modes, as is shown in Fig 10. Here propagation takes place by “hopping” from defect to defect, very much like tunneling through a succession of potential wells. Full transmission was observed from 11.5 to 12.6 GHz for both the straight and bent tunneling wave guides shown in Fig. 10. The efficiency of these so-called “coupled cavity waveguides” is reduced by structural imperfections. In a previous publication³⁰, Ozbay and co-

workers have shown that very precise defects can be created in alumina band-gap materials by use of laser machining.

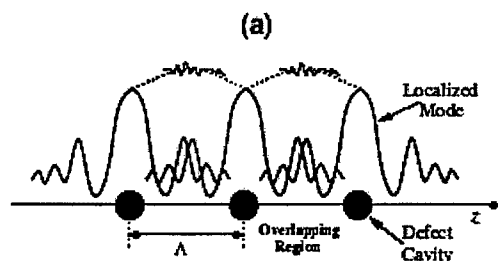


Fig 10 – (a) Schematics of propagation of photons by hopping between the coupled evanescent defect modes. The overlap of the defect modes is large enough to provide propagation of the EM waves along tightly confined cavity modes.

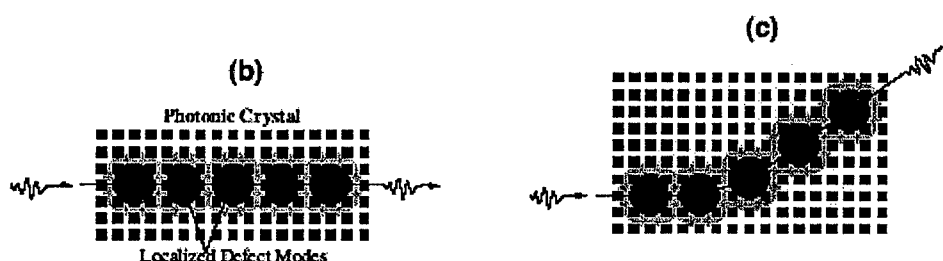


Fig 10 – (b) A mechanism to guide light through localized defect modes in photonic crystals. (c) Bending of the EM waves around sharp corners.

Ozbay *et al* have also shown that highly directional radiation can be obtained from radiation sources embedded within a band-gap crystal³¹. They observed that the radiation pattern from a monopole antenna embedded within a band-gap crystal is narrowest at the upper band edge, and that the radiation pattern is sensitive to the number of layers in the photonic crystal structure, with the optimum crystal size different for different operating frequencies.

Other applications of band-gap materials in microwave devices include construction of high-Q resonators³² and wide field-of-view spectral filters³³. In Ref 31, the authors show that a narrow-band spectral filter with a wide field of view can be constructed by stacking silicon gratings separated by air gaps to form a photonic crystal, and then inserting a defect layer in the center of the stack, which is similar to the grating layers, but with a different period and thickness. When the defect layer period is twice that of the grating layers, the center frequency of the filter is essentially constant over a $\pm 60^\circ$ range of angle of incidence. For comparison, when the defect period equals the grating period, the center frequency varies by 5% over the field of view, which is 4 times the filter bandwidth. This approach could enhance the sensitivity of wide-field microwave detectors.

An extensive review of microwave and mm-wave applications of electronic band-gap materials was recently published by Peter de Maagt *et al* of the European Space Agency³⁴. They discuss applications to array antennas, high precision GPS, mobile telephony, wearable antennas and diplexing antennas. They point out that since most fundamental components will soon be

available using band-gap technology, "a fully integrated receiver could be developed ... and true integration of active and passive band-gap components can now begin to materialize." Of the several important applications for band gap structures that have been identified and demonstrated, the one nearest to practical use is for conformal antennas, making use of a high-impedance ground plane. Other variants on antenna design attractive for near-term application are highly steerable antennas and antennas embedded in clothing³⁵. Fabrication of microwave band-gap structures is attractively simple, and the capacitance and inductance of individual elements can be tailored easily. Band-gap structures are compatible with millimeter wave integrated circuits.

IV. Terahertz Applications

The term, *Terahertz Radiation*, refers to the portion of the electromagnetic spectrum between 300 GHz and 3 THz³⁶ (100-1000 μm). This region of the spectrum has not been exploited until recently, mainly because of strong water absorption over much of the frequency range, and a lack of suitable sources and detectors. There has been some scientific interest in THz spectroscopy, however. Most simple molecules have strong rotational absorption lines in this region. It is also a region of great interest to astronomers, since the radiation from interstellar dust is well approximated by a 30 K black body spectrum, which peaks at about 100 μm . Currently, THz devices are under investigation for medical imaging applications, although the applications are limited by the prevalence of water in tissue. The primary applications are in dentistry and dermatology³⁷.

The scale length of Terahertz devices simplifies the problems of fabrication and assembly for photonic crystal structures. Devices can be assembled using well-developed MEMS techniques, and can be compact and highly integrated. Many of the applications considered parallel those in the microwave region, including improving the directionality of antennas, both in transmission and in imaging arrays. DeMaagt et al³⁸ report on the improved directionality of a dipole antenna operating at 500 GHz when mounted on a "woodpile" photonic crystal with a 3-dimensional bandgap extending from 480-540 GHz. They measured improvement from 2 dB directivity for an air-suspended dipole to 11 dB for the same dipole backed with a photonic crystal. The entire device was approximately six mm^2 in area. The ultimate objective is to assemble such devices into an imaging array.

A recent Japanese paper³⁹ describes a different way in which photonic crystals can enhance the process of THz generation. A common method of generating THz radiation is by beating two single-mode lasers operating with a THz difference frequency on a photoconductive antenna⁴⁰. The Japanese group embedded the photoconducting antenna between two photonic crystal structures. The embedded antenna achieved a peak emission intensity of more than twice that of a bare antenna. Strong enhancement was observed near the band edge of the photonic crystal, due to the high density of states at that frequency.

As in the microwave range, metallic elements can be used with THz devices. A Scottish research group⁴¹ has developed a tunable metallic photonic crystal filter for THz applications that consists of an array of movable metallic grids. Tuning is achieved by moving alternate grids sideways, changing the transverse periodicity of the array. This research is also interesting because it demonstrates some of the manufacturing techniques that can be employed in the THz and mm-wave regime. The first prototype⁴² of this filter was fabricated from sheets of aluminum alloy machined to a thickness of 500 μm . The cross-sectional area of the filter, including mechanical

supports, was 60mm x 40mm, with a transverse grid spacing of 1.8 mm. This device was tested at 70-110 GHz (mm-wave), and demonstrated tunability of the pass-band over a range of 3.5 GHz, with an insertion loss of 1.1-1.7 dB.

The authors then fabricated and tested a similar device, but manufactured from gold-coated silicon, using conventional MEMS techniques. Since the skin depth of gold at the operating frequency (70-150 GHz) is about 0.25 μm , a coating thickness of 1.2 μm was sufficient. This device showed tunability over a range of 7 GHz, with an insertion loss of 1 dB or less over the operating range. The authors comment that the use of MEMS fabrication techniques allow the construction of devices operating at higher frequencies (1-5 THz), where conventional machining techniques cannot be used. Their work also demonstrates the value of prototyping at lower frequencies.

A group at Tohuko University has recently demonstrated a novel method of fabricating photonic crystals for THz applications⁴³. They fabricated 300 μm -diameter copper spheres, and packed them into an fcc structure on a graphite base. The spheres were lightly sintered to form "necks" between adjacent spheres, constructing a three-dimensional template for an inverse photonic crystal. The interstitial spaces in the template were filled with a dielectric epoxy resin. After the resin was cured, the copper spheres were etched away, leaving a regular array of air holes in the epoxy matrix. The resulting structure exhibited a 160-GHz-wide stop band around 500 GHz in the [111] direction.

AFOSR has sponsored research on integrated optics for THz devices, especially at the high frequency end of the THz range. A group at the University of Delaware has demonstrated the use of a planar photonic crystal waveguide to create a compact integrated optics device operating at 30 THz (10 μm)⁴⁴. A waveguide was created by leaving a solid stripe through the center of a two-dimensional photonic crystal, as is shown in Fig. 11. Transmission was tested using a CO₂ laser operating at frequencies from 10.1 μm to 10.7 μm (28.0 – 29.7 μm), and was also modeled using a 3D-Finite-Difference-Time-Domain (FDTD) method⁴⁵. Both the measured and calculated transmission are shown in Fig 12. The scatter in the experimental data is attributed partly to imperfections in the fabrication process, and partly to possible variations in the insertion loss as the input laser is tuned from line to line. The gap in data from 28.6 to 29.0 THz is due to the unavailability of laser lines at those frequencies.

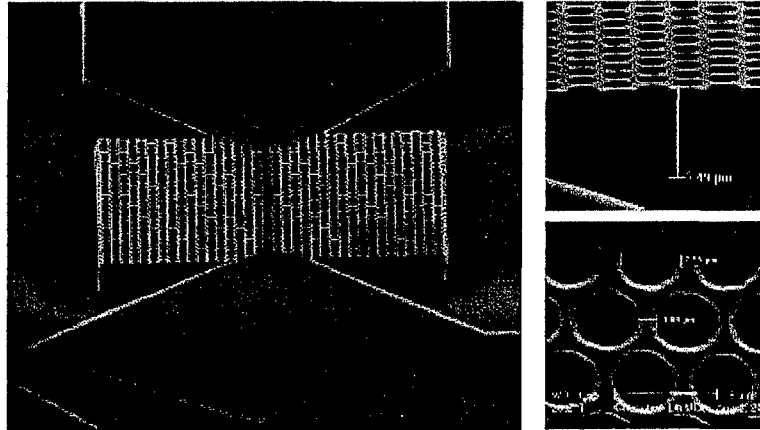


Fig. 11 –

(Left) SEM picture of photonic crystal waveguide. Total length = 120 μm ; width = 100 μm .

(right) SEM pictures of side and top views of the waveguide. Thickness = 9.49 μm ; hole diameter = 2.95 μm .

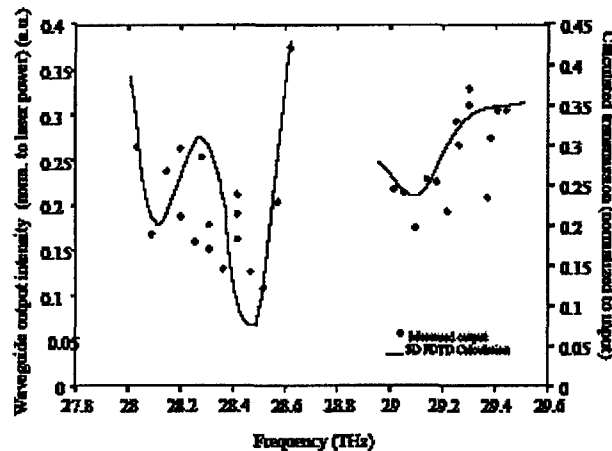


Fig. 12 – Calculated and experimentally measured transmittance spectra of 2-D photonic crystal waveguide.

Although photonic crystal structures are promising for use in sources, detectors, filters, and waveguides in THz systems, they must be evaluated in comparison to competing technologies. A wide variety of THz sources have been developed⁴⁶, including free-electron lasers, molecular lasers, quantum cascade lasers, and backward-wave oscillators. The most widely used sources of pulsed THz radiation are laser-driven emitters based on frequency down-conversion from intense sub-picosecond laser pulses. Continuous THz radiation can be generated by beating two frequency-offset laser beams on a photoconductor, as was described in Ref. 20. Recent research has also emphasized the use of surface plasmons in THz devices. For example, Wang and Mittleman⁴⁷, at Rice University have demonstrated waveguiding of THz radiation along a bare,

stainless-steel wire with low attenuation and negligible group velocity dispersion. Metamaterials⁴⁸ comprising discrete circuit elements also hold out great promise for application in the THz frequency range, and may suffer less from significant group dispersion effects than those composed of photonic crystal structures.

Terahertz radiation represents a new area of physics and engineering research. Unlike the microwave regime, an extensive body of technology does not already exist for THz use, so new approaches and devices do not face the same barriers to entry. The physical scale of photonic crystal structures in the THz range is commensurate with the use of established MEMS fabrication techniques. It is very likely that in certain applications, especially those in which broad bandwidth is not required, photonic crystal devices will find significant specialized applications for THz devices. In 2002, the European Space Agency (ESA) launched a multi-laboratory project called "Star Tiger" to develop Thz imaging technology based on the use of photonic crystal mirrors. The project successfully produced a prototype imaging system on a chip⁴⁹. The THz waves were detected by heterodyning the signal down to radio frequencies, due to the lack of direct detectors. ESA has continued research on THz applications of band-gap materials, and is currently developing THz imaging arrays⁵⁰.

IV. Elastic, Acoustic and Ultrasonic Applications

Shortly after the publication of the first few papers on Photonic Crystals (Ref. 6,7), research began on applying band-gap structures to acoustic and elastic waves⁵¹. The literature on these applications is nowhere as extensive as on photonic applications, and much of the research is carried out outside the US, with active groups in Spain, France, Taiwan, Hong Kong, Greece, South Korea and Canada. Acoustical experiments do not require as sophisticated methods or materials as microwave or optical experiments. A Spanish research group⁵² constructed a "phononic crystal" by hanging an array of aluminum cylinders from a rotating support, and driving a speaker with a frequency generator and observing the transmission with conventional microphones. Experiments were conducted at audio frequencies (250-3500 Hz) and attenuation and phase delay were observed. Several configurations were examined, with rod diameters varying from 1 to 4 cm, and lattice spacings of 5.5 and 11 cm. in square and hexagonal lattices. The experimental results showed the expected agreement with theory, with strong attenuation within the band gap (although the data was quite noisy) and anomalous dispersion at the band edges. In addition, the authors observed "deaf bands," which were regions of frequency where sound in certain directions was trapped inside the structure for reasons of symmetry.

As in the microwave regime, the design space for elastic band gap structures is very large, with several parameters that can be chosen to determine the structure's response. Whether in two or three dimensions, the location and extent of the stop bands depends on the dimensions, sound speeds and densities of the materials used, and the internal structure of the lattice components. Thus, in an array of cylinders, the cylinders can be solid or have a hollow core, which can be filled with a separate material, or the outside of the cylinder can be coated with a disparate material. Khelif *et al*⁵³ modeled a two-dimensional band gap structure of steel cylinders in water, and calculated the transmission properties of this lattice, comparing results with solid cylinders to those from hollow cylinders of various wall thickness. With solid cylinders, the band gap extended from 100 kHz to 200 kHz. With hollow cylinders, the upper band edge was extended to 220 kHz, and a narrow pass band was introduced within the band gap, due to a resonance within the cylinders that interferes with the wave cancellations within the entire lattice. According to

their calculations, the frequency of the narrow pass band can be tuned by varying the ratio of the cylinder wall thickness to the cylinder diameter.

Researchers in Hong Kong previously carried out a related experiment⁵⁴ in which they constructed a lattice of lead spheres, coated with silicone rubber, embedded in an epoxy matrix (See Fig.12).

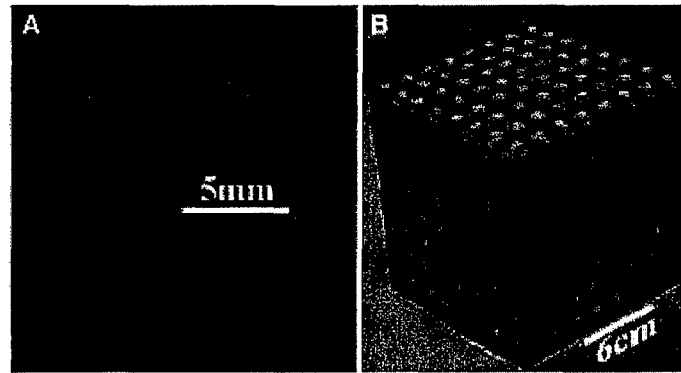


Fig. 12 – A) cross section of a coated lead sphere. B) 8x8x8 Sonic Crystal

Transmission through the crystal was measured at frequencies from 0 to 2 kHz. The band structure and transmission were calculated for comparison, and reasonable agreement with experiment was obtained (see Fig 13).

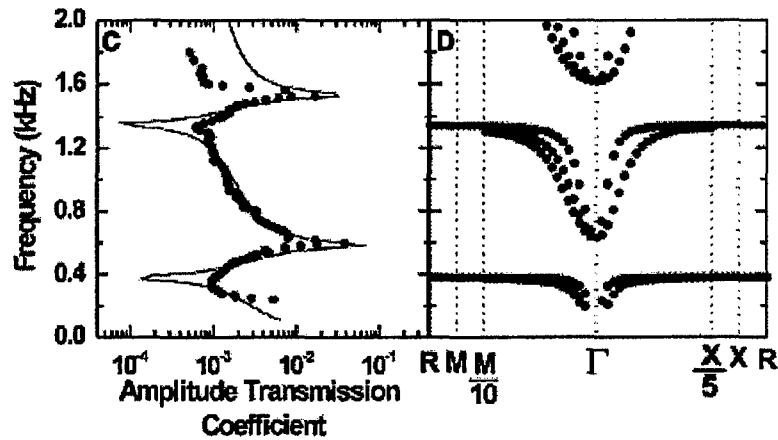


Fig. 13 –

C) Comparison of measured (dots) and calculated (solid line) values of transmission vs. frequency.

D) Calculated band structure of a simple cubic array of coated spheres, from 0.2 to 2 kHz.

In Fig. 13, the band structure is shown for the [110] direction (left of Γ -point) and the [100] direction (right of Γ -point). Since the crystal is completely solid (no liquids or gases) it can support shear waves, so three modes (two transverse and one longitudinal) are seen in the [110] direction. In the [100] direction, the transverse modes are degenerate.

The bands at 380 and 1350 Hz correspond to wavelengths much longer than the lattice spacing. At 500 Hz (mid-band) the wavelength of a longitudinal wave in epoxy is about 5 m. The observed bands are well below the frequencies characteristic of the lattice spacing of 1.55 cm., and are attributed to the motions of the lead balls within the rubber coatings. The lower band represents the "acoustic" mode, in which the lead spheres vibrate in phase, with the rubber coatings providing the restoring force, and the upper band represents the "optical" mode, in which adjacent spheres vibrate out of phase, compressing the rubber between them. The key conclusion of this paper is that the frequency of these sub-bands only depends on the thickness of the coatings. Mixtures of different coating thicknesses could provide broad regions of low transmission across the acoustic spectrum, in structures that are much smaller than acoustical wavelengths. The authors propose to apply this technology to the construction of compact acoustic barriers.

A Spanish research group has carried out an extensive analysis of such ternary (three-component) systems⁵⁵ in two dimensions. Their analysis confirms the calculations of Ref. 53, and they propose a mechanical analogue consisting of a chain of mass-and-spring resonators, with a pendulum attached to each mass. The dispersion relation of such a system shows the same features as the ternary photonic crystal, with sub-bands whose frequency is determined by the parameters of the locally resonant structures. They also point out that while the local resonance determines the frequency of the sub-bands, the local resonators are weakly coupled through the lattice, so that the propagation characteristics near the local resonance are somewhat sensitive to the lattice structure and symmetry.

A variant of a ternary system has been proposed by another group in Hong Kong⁵⁶. Their computations show that the absolute band gap in a hexagonal two-dimensional lattice consisting of aluminum cylinders in an epoxy matrix can be greatly expanded by interspersing air-filled columns between the aluminum cylinders to suppress transverse shear modes. This approach has the advantage of reducing the weight of the structure while improving its performance as a sound barrier.

Band gap materials are also promising for application to ultrasonics. At ultrasonic frequencies in the range from 0.1-1.0 MHz, wavelengths range from 0.3 to 3 mm in air, 0.1 to 1 cm in water, and 0.5 to 5 cm in steel or aluminum, so band gap materials for ultrasonics are of comparable scale to those used for microwave devices. Essentially all of the attributes of band gap materials observed at microwave and optical frequencies have been reproduced using ultrasonic acoustic and elastic waves. For example, Khelif and colleagues⁵⁷ have reported the guiding and bending of acoustical waves at frequencies of 220-340 kHz in a 2-dimensional lattice of steel rods immersed in water. Wave guiding was introduced by removing one or two rows of steel rods, and in one case, creating a z-shaped path through the crystal. With one row removed, they observed single mode propagation over a pass band from 250 kHz to 325 kHz, but with two rows removed, two modes were included in the waveguide pass band. Losses through the z-shaped path were less than 5 dB over 70% of the full pass band. Other phenomena that have been observed at ultrasonic frequencies include tunneling within the stop band⁵⁸ and creation of an acoustical lens due to the effective negative index in regions of strong group velocity dispersion⁵⁹. In the latter case, the authors constructed a phononic crystal by stacking tungsten carbide beads in water. The dimensions were chosen to block transmission of ultrasound at about 1 MHz. There is a narrow region of strong anomalous dispersion at the upper edge of the band gap, where an effective "negative index" is found. Experimental results are shown in Fig. 14. At 1.57 MHz, the sound waves are strongly focused, while at 1.60 Mhz, no focusing is observed.

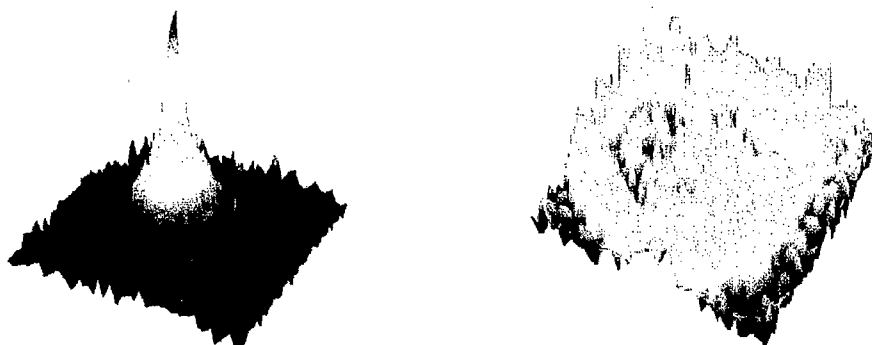


Fig. 14 – Focusing is observed at 1.57 MHz (left) but not at 1.60 MHz (right).

A novel experiment demonstrating the universal nature of wave phenomena was carried out by Robertson *et al*⁶⁰, who reported sound wave propagation at a velocity one-fourth the nominal speed of sound in air. Sound waves in the range of 1-2 kHz were propagated through an acoustical wave guide consisting of alternating sections of pipe with different radii. The variation in diameter gave rise to periodic reflections, setting up a one-dimensional band-gap structure. A defect was introduced by placing a section of pipe of twice the length of the other pieces in the center of the wave guide, creating a narrow pass band in the center of the band gap. Due to the strong dispersion in the vicinity of the narrow pass band, the group velocity is significantly reduced. The authors propagated an acoustical pulse of sufficient length that its frequency spectrum fell entirely within the defect-generated narrow pass band. By measuring the difference in the pulse propagation time between an unmodulated wave guide and the periodic structure, the authors found that the pulse was slowed to one-fourth of nominal sound speed in the defect section of the waveguide. They propose that this result is analogous to the light speed reduction observed in resonant atomic vapors⁶¹.

Elastic waves also propagate along a free surface. Two recent papers discuss the application of band gap structures to the attenuation of surface elastic waves. In Spain, Professor Meseguer and colleagues⁶² have studied the propagation of Rayleigh waves across a two-dimensional band gap structure created by drilling a periodic lattice of cylindrical holes in the surface of a marble quarry. They chose to do their experimentation in a marble quarry because it presents wide areas of flat surface, the marble layer is much thicker than the depth of penetration of the surface wave, and it provides a good simulation of earthquake-generated waves on the earth's surface. The lattice consisted of 6-cm diameter holes in both hexagonal and triangular arrays, with lattice spacing of 14 cm. Surface waves were excited by striking the surface with a 1.27-cm diameter steel ball. The excitation spectrum was measured over a frequency range up to 20 kHz. The recorded seismogram showed the presence of longitudinal and transverse (P and S) bulk waves, followed by a sharp Rayleigh peak. The attenuation spectrum showed relatively sharp peaks at the expected Bragg frequencies for this lattice spacing, and also showed broad attenuation regions at low frequencies. The authors discussed using this kind of band-gap structure as a barrier against seismic waves, but it is apparent that the size and scale of the structure required rendered it impractical.

A Korean group⁶³ proposed the use of band-gap arrays for protection of coastal areas against ocean waves. They measured the attenuation of water waves by both a hexagonal and triangular

2-dimensional lattice, at frequencies up to 10 Hz. 20 to 30 dB attenuation was observed over much of the frequency range, although the authors say that a more extensive array would lead to higher attenuation. They propose that a hexagonal lattice with a spacing of 10m would provide protection against most coastal water waves, and would be more eco-friendly than massive solid barriers.

Band-gap structures have many positive attributes for application to acoustic and elastic waves. Readily available materials provide a wide range of parameters, especially mass density and sound speed. Thus, "high contrast" materials can be used to make compact structures. The scale length of acoustic and elastic wave devices is convenient for fabrication, especially for ternary structures, which offer real advantages for extending the stop bands and inserting narrow pass bands. The use of fluid materials can effectively eliminate shear waves, simplifying the structures.

At acoustical frequencies, the use of band gap materials for noise barriers has been extensively studied. Ternary systems offer some possibilities of providing high attenuation at low frequencies, while keeping the barrier at a reasonable size. However, conventional sound-absorbing materials are very effective, and it will be difficult to displace them for most applications. As in the microwave regime, band-gap materials are proposed for use in ultrasonic systems as filters, wave guides, add-drop multiplexers, lenses, and components in detectors and transmitters. At ultrasonic frequencies, band-gap structures may be the preferred approach for some applications, especially those in which frequency selectivity is required.

V. Summary and Conclusions

Research on band-gap materials has been active and growing since its start in 1987. Although a large fraction of the research is aimed toward optical applications, microwave, THz and acoustical applications have been extensively studied, in part due to the fact that construction of band gap materials at these wavelengths is easier and less expensive. Furthermore, as we have shown, there are valid applications of band-gap structures and concepts throughout the electromagnetic and acoustic spectra. The one application that stands out as closest to practical application is in the area of microwave and mm-wave antenna design, where the suppression of surface waves can lead to more compact conformal designs.

After nearly twenty years of study, the scientific community has a much clearer picture of the possibilities and limitations of band-gap materials. Research is still flourishing, and innovation is still taking place, although there appears to be a reduction in funding for new projects. Research in this field provides an excellent training ground for students in physics and engineering, since it combines elements of applied mathematics, wave theory and materials science with practical applications. The field has attracted university research groups all around the world.

At present, apart from the antenna applications, there does not seem to be a "killer application" for band-gap materials. However, there are several areas of application, especially in THz devices, microwave integrated circuits, and possible ultrasonics, where new components and devices based on these structures will become part of the inventory. As we have shown, there is great flexibility in designing band-gap structures, with widely varying materials properties and configurations to choose from. At the wavelengths applicable to microwave and acoustical

devices, additional flexibility is provided by using structured elements or ternary configurations, to combine the effects of local resonances with the overall symmetry properties of the crystal.

VI. Acknowledgements

I would like to thank the following people for instructive and illuminating discussions: Dr. Peter deMaagt, (European Space Agency), Professor Yahya Rahmat-Samii (Univ. of California in Los Angeles), Professor Kevin Malloy (Univ. of New Mexico), Dr. Daniel Sievenpiper (Hughes Research Laboratory), and Professor Eli Yablonovich (Univ. of California in Los Angeles). I would also like to thank the following staff members of the Air Force Weapons Laboratory in Albuquerque for discussions of the possible relevance of band-gap structures to Air Force programs: Dr. Harro Ackermann, Dr. Anastasias Gavrielides, Dr. Concetto Giuliano, Dr. Vern Schlie and Dr. Peter Turchi. The support of Dr. Jack Agee and the U.S. Air Force Office of Scientific Research is gratefully acknowledged.

VII. References

- ¹ L.Brillouin, *Quantenstatistik*, Springer-Verlag, Berlin (1931).
- ² L.Brillouin, *Wave Propagation in Periodic Structures*, McGraw-Hill Book Company, New York (1946).
- ³ J.M.Ziman, *Electrons in Metals*, Taylor & Francis Ltd., London (1962).
- ⁴ M. Born and E. Wolf, *Principles of Optics*, Pergamon Press, Oxford, sixth edition (1993).
- ⁵ R. Kingslake, *History of the Photographic Lens*, Academic Press, Boston, (1989).
- ⁶ E. Yablonovich, "Inhibited spontaneous emission in solid-state physics and electronics", *Phys. Rev. Lett.* **58**, 2059 (1987).
- ⁷ E. Yablonovitch, and T.J.Gmitter, "Photonic Band Structures: The face-centered cubic case," *Phys. Rev. Lett* **63**, 1950, (1989).
- ⁸ T.A.Birks, J.C.Knight and P.St.J.Russell,, "Endlessly single-mode photonic crystal fiber," *Opt. Lett.* **22**, 961 (1987).
- ⁹ J. Dowling, <http://baton.phys.lsu.edu/~jdowling/pbgbib.html#R>
- ¹⁰ F. Bloch, *Zeitschrift fur Physik* **52**, 555 (1928).
- ¹¹ J.D.Joannopoulos, R.D.Meade, and J.N.Winn, *Photonic Crystals*, Princeton Univ. Press, Princeton, NJ (1995)
- ¹² R.deL.Kronig and W.G.Penney, *Proc. Royal Soc.* **130**, 499 (1931)
- ¹³ S. Mishra and S. Satpathy, "One-dimensional photonic crystal: The Kronig-Penney Model," *Phys. Rev. B* **68**, 045121 (2003).
- ¹⁴ B.Gralek, S.Enoch and G.Tayeb, "Anomalous refractive properties of photonic crystals," *J. Opt. Soc. Am. A* **17**, 1012-1020 (2000)
- ¹⁵ S.Enoch, G.Tayeb and B.Gralak, "The richness of the dispersion relation of electromagnetic bandgap materials," *IEEE Transactions On Antennas And Propagation*, **51**, 2659-2666 (2003)
- ¹⁶ *Progress in Electromagnetics Research*, PIER **41**, (A. Priou and T. Itoh, Editors), Cambridge, MA (2003). Each chapter of this book can be found on the Web at <http://cetaweb.mit.edu/pier/pier41/pier41.html>.
- ¹⁷ E.N.Economou and M.M.Sigalas, "Classical wave propagation in periodic structures: Cermet versus network topology," *Phys. Rev. B* **48**, 13 434-13 438 (1993)
- ¹⁸ D. Sievenpiper, L.Zhang,R.F.J.Broas, N.G.Alexopolous, and E. Yablonovitch, "High-impedance electromagnetic surfaces with a forbidden frequency band," *Transactions on Microwave Theory and Techniques* **47**, 2059-2074 (1999)
- ¹⁹ E. Yablonovitch, Personal Communication.
- ²⁰ R. Gonzalo, P.J.I.de Maagt, M.Sorolla,"Enhanced patch antenna performance by suppressing surface waves using photonic band-gap structures," *IEEE Transaction on Microwave Theory and Techniques* **47**, 2131-2138 (1999)
- ²¹ J.S.Colburn and Y.Rahmat-Samii, "Patch antennas on externally perforated high dielectric constant substrates," *IEEE Transaction on Antennas and Propagation*, **47**, 1785-1794 (1999)
- ²² R. Gonzalo, G. Nagore and P. de Maagt, "Simulated and measured performance of a patch antenna on a 2-dimensional photonic crystal substrate," *Progress in Electromagnetics Research*, PIER **41**, (A. Priou and T. Itoh, Editors), 257-269, Cambridge, MA (2003). See Note 16.

- ²³ Q.C.Lin, F.M.Zhu, and S.L.He, "A new photonic bandgap cover for a patch antenna with a photonic bandgap substrate," *Journal of Zhejiang University SCIENCE*, **5**, 269-273 (2004)
- ²⁴ D.F.Sievenpiper, J.H.Schaffner, H.J.Song, R.Y.Loo, and G.Tangonan, "Two-dimensional beam steering using an electrically tunable impedance surface," *IEEE Transactions On Antennas And Propagation*, **51**, 2713-2722 (2003)
- ²⁵ F.Yang and Y.Rahmat-Samii, "Microstrip antennas integrated with electromagnetic band-gap (EBG) structures: a low mutual coupling design for array applications," *IEEE Trans. On Antennas and Propagation*, **51**, 2936-2946 (2003)
- ²⁶ C.C.Chang, Y.Qian and T.Itoh, "Analysis and applications of uniplanar compact photonic bandgap structures," *Progress in Electromagnetics Research*, **PIER 41**, (A. Priou and T. Itoh, Editors), 211-235, Cambridge, MA (2003). See Note 16.
- ²⁷ T.L.Wu, Y.H.Lin and S.T.Chen, "A novel power plane with low radiation and broadband suppression of ground bounce noise using photonic bandgap structures," *IEEE Microwave and Wireless Components Letters*, **14**, 337-339 (2004)
- ²⁸ E.Ozbay, B.Temelkuran and M.Bayindir, "Microwave applications of photonic crystals," *Progress in Electromagnetics Research*, **PIER 41**, (A. Priou and T. Itoh, Editors), 185-209, Cambridge, MA (2003). See Note 16.
- ²⁹ E. Ozbay, "Layer-by-layer photonic band-gap crystals: from microwave to far infrared," *Journ. Opt. Soc. Am.* **B13**, 1945 (1996)
- ³⁰ E.Ozbay, G.Tuttle, J.S.McCalmont, M.Sigalas, R.Bigwas, C.M.Soukoulis and K.M.Ho, "Laser-micromachined millimeter-wave photonic band-gap cavity structures," *Appl. Phys. Lett.* **67**, 1969-1971 (1995).
- ³¹ I.Bulu, H.Caglayan and E.Ozbay, "Highly directive radiation from sources embedded inside photonic crystals," *Appl. Phys. Lett.* **83**, 3263-3265 (2003)
- ³² A.Serpenguzel, "Metallodielectric photonic crystals and resonators," *Proc. of SPIE Vol.* **5000**, 297-301 (2003)
- ³³ R.J.Blaikie, T.D.Drysdale, H.M.H.Chong, I.G.Thayne and D.R.S.Cumming, "Wide field-of-view photonic bandgap filters micromachined from silicon," *Microelectronic Engineering* **73-74**, 357-361 (2003)
- ³⁴ P. de Maagt, R.Gonzalo, Y.C.Vardaxoglou, J.-M.Baracco, "Electromagnetic bandgap antennas and components for microwave and (sub)millimeter wave applications," *IEEE Trans. Antennas and Propagation* **51**, 2667-2677 (2003)
- ³⁵ Dan Sievenpiper, Personal Communication
- ³⁶ P.H. Siegel, *Terahertz Technology*, *IEEE Transactions on Microwave Theory and Techniques*, 910-928 (2002)
- ³⁷ K. Humphreys, J.P.Loughran, M.Gradziel, W. Lanigan, T. Ward, J.A. Murphy, and C. O'Sullivan, "Medical applications of terahertz imaging: a review of current technology and potential applications in biomedical engineering," 26th Annual International Conference of the IEEE Engineering in Medicine and Biology Society, 1-5 Sep. 2004, San Francisco, CA.
- ³⁸ R. Gonzalo, I. Ederra, C.M.Mann and P.deMaagt, "Radiation properties of terahertz dipole antenna mounted on photonic crystal," *Electronics Letters* **37**, 613-614, (2001)
- ³⁹ M.Iida, M.Tani, K.Sakai, M.Watanabe, S.Katayama H.Kondo, H. Kitahara, S. Kato and M.W.Takeda, "Emission from planar defect modes excited with surface modes in three-dimensional photonic crystals," *Phys. Rev.* **B69**, 245119-245124 (2004)
- ⁴⁰ E.R.Brown, K.A.McIntosh, K.B.Nichols, and C.L. Dennis, "Photomixing up to 3.8 THz in low-temperature-grown GaAs," *Appl. Phys. Lett.* **66**, 285-287 (1995)
- ⁴¹ T.D.Drysdale, G.Mills, S.M.Ferguson, R.J.Blaikie, and D.R.S.Cumming, "Metallic tunable photonic crystal filter for terahertz frequencies," *J. Vac. Sci. Technology B* **21**, 2878-2882 (2003)
- ⁴² T.D.Drysdale, R.J.Blaikie, and D.R.S.Cumming, "A tunable photonic crystal filter for terahertz frequency applications," *Proceedings of the SPIE* **5070**, 89-97 (2003)
- ⁴³ K.Tagaki, K.Seno, and A.Kawasaki, "Fabrication of a three-dimensional terahertz photonic crystal using monosized spherical particles," *Appl. Phys. Letters* **85**, 3681-3683 (2004).
- ⁴⁴ C.Lin, C.Chen, G.J.Schneider, P.Yao, S.Shi, A.Sharkawy, and D.W.Prather, "Wavelength scale terahertz two-dimensional photonic crystal waveguides," *Optics Express* **12**, 5723-5728 (2004)
- ⁴⁵ K. Shlager and J. Schneider, "A selective survey of the finite-difference time-domain literature," *IEEE Antennas and Propagation Magazine*, vol. 37, pp. 39-56, 1995.
- ⁴⁶ G.P.Gallerano and S.Biedron, "Overview of terahertz radiation sources," *Proceedings of the 21st International FEL Conference*, 216-221, To be published online at <http://www.JACoW.org> (2005)
- ⁴⁷ K. Wang and D.M.Mittleman, "Metal wires for terahertz wave guiding," *Nature* **432**, 376-379 (2004)
- ⁴⁸ D.R.Smith, J.B.Pendry and M.C.K.Wiltshire, "Metamaterials and negative refractive index," *Science* **305**, 788-792 (2004)
- ⁴⁹ D. Clery, "Brainstorming their way to an imaging revolution," *Science* **297**, 761-763 (2002)
- ⁵⁰ Dr. Peter deMaagt, Personal Communication.

- ⁵¹ M.M.Sigalas and E.N. Economou, "Elastic and acoustic wave band structure," J. Sound Vibration, **158**, 377-382 (1992)
- ⁵² C.Rubio, D.Caballero, J.V.Sanchez-Perez, R.Martinez-Sala, J.Sanchez-Dehesa, F. Meseguer and F. Cervera, "The existence of full gaps and deaf bands in two-dimensional sonic crystals," Journal of Lightwave Tech. **17**, 2202-2207 (1999)
- ⁵³ A.Khelif, P.A.Deymier, B.Djafari-Rouhani, J.O.Vasseur, and L.Dobrzynski, "Two-dimensional phononic crystal with tunable narrow pas band: Application to a waveguide with selective frequency," J. Appl. Phys. **94**, 1308-1311 (2003)
- ⁵⁴ Z.Liu, X.Zhang, Y.Mao, Y.Y.Zhu, Z. Yang, C.T.Chan and P.Shang, "Locally resonant sonic materials," Science **289**, 1734-1736 (2000)
- ⁵⁵ C. Goffaux and J.Sanchez-Dehesa, "Two-dimensional phononic crystals studied using a variational method: Application to lattices of locally resonant materials," Phys. Rev. B **67**, 144301-1 to 144301-10 (2003)
- ⁵⁶ Y.Lai and Z.Q.Zhang, "Large bandgaps in elastic phononic crystals with air inclusions," Appl. Phys. Lett. **83**, 3900-3902 (2003)
- ⁵⁷ A.Khelif, A.Choujaa, S.Benchabane, B.Djafari-Rouhani and V.Laude, "Guiding and bending of acoustic waves in highly confined phononic crystal waveguides," App. Phys. Letters **84**, 4400-4402 (2004)
- ⁵⁸ S.Yang, J.H.Page, Z.Liu, M.L.Cowan, T.Chan and P.Sheng, "Ultrasound tunneling through 3D phononic crystals," Phys. Rev. Letters **88**, 104301-1 to 104301-4 (2002)
- ⁵⁹ S.Yang, J.H.Page, Z.Liu, M.L.Cowan, T.Chan and P.Sheng, "Focusing of sound in a 3D phononic crystal," Phys. Rev. Letters **93**, 024301-1 to 024301-4 (2004)
- ⁶⁰ W.M.Robertson, C.Baker and C.B.Bennett, "Slow group velocity propagation of sound via defect coupling in a one-dimensional acoustic band gap array," Am. J.Phys **72**, 255-257 (2004)
- ⁶¹ L.V.Hau, S.E.Harris, Z. Dutton and C.H.Behroozi, "Light speed reduction to 17 meters per second in an ultracold atomic gas," Nature **397**, 594-598 (1999)
- ⁶² F.Meseguer, M.Holgado, D.Caballero, N.Benaches, C.Lopez, J.Sanchez-Dehesa and J.Llinares, "Two-dimensional elastic bandgap crystal to attenuate surface waves," IEEE Journ. Of Lightwave Technology **17**, 2196-2201 (1999)
- ⁶³ T.S.Jeong, J.E.Kim, H.Y.Park and I.W.Lee, "Experimental measurement of water wave band gaps" Appl. Phys. Letters **85**, 1645-1647 (2004)

REPORT DOCUMENTATION PAGE

AFRL-SR-AR-TR-05-

0419

Public reporting burden for this collection of information is estimated to average 1 hour per response, including the time for reviewing instructions, searching existing data sources, gathering the required data, completing and reviewing this collection of information. Send comments regarding this burden estimate or any other aspect of this collection of information, including suggestions for reducing this burden, to Washington Headquarters Services, Directorate for Information Operations and Reports (0704-0111), Paperwork Project, Washington, DC 20540-6001. Respondents should be aware that notwithstanding any other provision of law, no person shall be subject to a penalty for failing to comply with a collection of information if it does not have a valid OMB control number. PLEASE DO NOT RETURN YOUR FORM TO THE ABOVE ADDRESS.

1. REPORT DATE (DD-MM-YYYY) 23-02-2005		2. REPORT TYPE Final Technical Report		3. DATES COVERED (From - To) Aug 04 thru Feb 05	
4. TITLE AND SUBTITLE Non-Optical Applications of Photonic Crystal Structures				5a. CONTRACT NUMBER FA9550-04-1-0456	
				5b. GRANT NUMBER	
				5c. PROGRAM ELEMENT NUMBER	
6. AUTHOR(S) Alexander J. Glass, Ph.D.				5d. PROJECT NUMBER	
				5e. TASK NUMBER	
				5f. WORK UNIT NUMBER	
7. PERFORMING ORGANIZATION NAME(S) AND ADDRESS(ES) Regents of the University of New Mexico, Office of Research Services Scholes Hall, Room 102 Albuquerque, NM 87131-6003				8. PERFORMING ORGANIZATION REPORT NUMBER 18255-F	
9. SPONSORING / MONITORING AGENCY NAME(S) AND ADDRESS(ES) USAF, AFR Air Force Office of Scientific Research 875 N. Randolph St, Ste 325, Rm 3112 Arlington, VA 22203-1768 NE				10. SPONSOR/MONITOR'S ACRONYM(S) USAF, AFRL, AFOSR/PK1	
				11. SPONSOR/MONITOR'S REPORT NUMBER(S)	
12. DISTRIBUTION / AVAILABILITY STATEMENT Approved for Public Release; Distribution Unlimited					
13. SUPPLEMENTARY NOTES					
14. ABSTRACT This study provides a comprehensive survey of current research on non-optical applications of photonic crystal concepts. Primary emphasis is placed on applications in the microwave (GHz), THz and acoustical regimes, including negative refraction and ultrasonics. Special attention will be devoted to research conducted outside the United States, which represents a significant portion of the relevant open literature. The study provides a summary of progress and problems remaining to be solved, and a discussion of possible Air Force applications of developments in non-optical photonic crystal research.					
15. SUBJECT TERMS Photonic crystals, periodic structures, band structure, Terahertz applications, band-gap materials					
16. SECURITY CLASSIFICATION OF:			17. LIMITATION OF ABSTRACT SAR	18. NUMBER OF PAGES 23	19a. NAME OF RESPONSIBLE PERSON Alexander Glass
a. REPORT Unclassified	b. ABSTRACT Unclassified	c. THIS PAGE Unclassified			19b. TELEPHONE NUMBER (include area code) 510 658-9847